

# Antiresonances in Molecular Wires

Eldon G. Emberly\* and George Kirczenow

*Department of Physics, Simon Fraser University, Burnaby, B.C., Canada V5A 1S6*

(July 8, 2018)

## Abstract

We present analytic and numerical studies based on Landauer theory of conductance antiresonances of molecular wires. Our analytic treatment is a solution of the Lippmann-Schwinger equation for the wire that includes the effects of the non-orthogonality of the atomic orbitals on different atoms exactly. The problem of non-orthogonality is treated by solving the transport problem in a new Hilbert space which is spanned by an orthogonal basis. An expression is derived for the energies at which antiresonances should occur for a molecular wire connected to a pair of single-channel 1D leads. From this expression we identify two distinct mechanisms that give rise to antiresonances under different circumstances. The exact treatment of non-orthogonality in the theory is found to be necessary to obtain reliable results. Our numerical simulations extend this work to multichannel leads and to molecular wires connected to 3D metallic nanocontacts. They demonstrate that our analytic results also provide a good description of these more complicated systems provided that certain well-defined conditions are met. These calculations suggest that antiresonances should be experimentally observable in the differential conductance of molecular wires of certain types.

PACS: 73.40.-c, 73.61.Ph, 73.23.-b

Typeset using REVTeX

---

\*e-mail: eemberly@sfu.ca copyright IOP 1999

## I. INTRODUCTION

There has been renewed interest recently in molecular wires,<sup>1</sup> stimulated in part by experimental work that has begun to explore possible ways of measuring the conductance of a single molecule.<sup>2–5</sup> Theoretically, electron transport in molecular wires has been studied by considering the transmission probability for electrons to scatter through the structure.<sup>3,6–10</sup> As with other mesoscopic systems, the electrical conductance  $G$  of the molecule is related to the transmission probability  $T$  at the Fermi level by the Landauer formula<sup>11</sup>  $G = \frac{e^2}{h} T$ .

As expected for mesoscopic systems with discrete energy levels connected to continuum reservoirs, molecular wires display resonances in the transmission probability. Another potentially important transport phenomenon that has been predicted in molecular wires is the appearance of antiresonances.<sup>7</sup> These are defined to be zeroes of the transmission and correspond to the incident electrons being perfectly reflected by the molecule. In molecular systems this phenomenon was first recognised in theoretical studies of electron transfer between donor and acceptor sites of a molecule.<sup>12–14</sup> At that time it was correctly attributed to interference effects between the different molecular orbitals through which the electron propagates. However, antiresonances have received less attention in the context of electrical conduction through molecular wires connected to metallic contacts and we address this topic theoretically in the present article.<sup>15</sup>

The occurrence of antiresonances has also been reported in other mesoscopic systems. They have been found in quantum waveguides<sup>16–22</sup> where the transmission displays resonance-antiresonance structure. These systems in the form of stub tuners have been shown to operate as electronic gates. Antiresonances have also been proposed to occur in double barrier resonant tunneling (DBRT) devices. There they have been explained using a Fabry-Perot model of the DBRT<sup>23</sup> and have also arisen in more sophisticated tight-binding calculations of the same structures<sup>24</sup>. In the above devices it is the wave nature of the electrons that leads to these interesting interference effects. Although the wave nature of the electrons is also the cause of antiresonances in molecular wires, it will be seen below that different mechanisms are responsible for their occurrence in the molecular systems.

We begin by considering a simple model of molecular wires exhibiting antiresonances that we solve analytically. We then proceed to investigate the robustness of the analytically predicted behaviour by studying more realistic models numerically.

Our analytic model of the molecular wire consists of a molecule attached to two ideal single-channel 1D leads. Electrons are incident from the left lead in only one propagating channel and scatter through the molecule to the single channel of the right lead. The electronic structure of the molecule is described as a discrete set of molecular orbitals which couple to the single mode leads. We show that in discussing molecular wire antiresonances it is important to take into account explicitly the fact that the atomic orbitals on neighbouring atoms overlap each other; in some of the systems that we consider antiresonances are only found if this non-orthogonality is included fully in the theory. In our analytic calculations the non-orthogonality is taken into account exactly by defining a new energy and overlap dependent Hamiltonian in a basis that is orthogonal and spans a new Hilbert space.<sup>15</sup> This switching of Hilbert spaces greatly simplifies the analytic solution of the present problem and should have broad applicability to other transport problems as well, whenever the mutual non-orthogonality of tight-binding states is important. It is an alternative to standard

orthogonalisation transformations such as the Wannier or Löwdin transformation. It has the advantages of being much simpler to implement and much more flexible than the Wannier transformation since it can be usefully applied to *all* systems described by tight binding models in contrast to the transformation to Wannier states that is useful mainly in the theory of crystalline solids. It also differs from the Löwdin transformation that is used in quantum chemistry which defines a new set of orthogonal atomic orbitals in terms of the original non-orthogonal atomic orbital set.<sup>25</sup> We solve the Lippmann-Schwinger equation in this new Hilbert space to find the transmission probability  $T$  of the electrons to scatter through the molecule. We derive a simple condition controlling where the antiresonances occur in the transmission spectrum. This condition only depends on the free propagator for the molecule and the energy- dependent couplings between the molecular orbitals and the ideal leads. For a molecule with  $N$  orbitals, the antiresonance condition predicts that there can be at most  $(N - 1) + 2$  antiresonances.

We then present numerical results for two more general molecular wire models in order to show how antiresonances might be observable in real systems. Our analytic model is applicable to  $\pi$  conjugated systems where the  $\pi$  orbitals are independent of the  $\sigma$  states that are also present in realistic systems. It is able to predict the energies at which antiresonances occur in our more sophisticated calculations. The first of these uses polyacetylene-like polymers for the two leads which are attached to a molecule that has a single  $\pi$  molecular orbital. This molecular wire exhibits a transmission antiresonance in the occupied  $\pi$  band of the leads.

Our second more realistic model is of a molecular wire bridging a mechanically controlled break junction in a metal wire. In this case the molecular wire consists of an “active” molecular segment connected to the two metal contacts by a pair of finite  $\pi$  conjugated chains. In this calculation we show how an antiresonance can be generated near the Fermi energy of the metallic leads. The differential conductance is calculated for this system using Landauer theory and the antiresonance is characterised by a dip in conductance. We find that for both of these calculations involving multi-mode leads our analytic theory of antiresonances has predictive power.

In Sec. II, we describe the method that we use to treat the non-orthogonality of atomic orbitals and present the solution to the Lippmann-Schwinger equation for our analytic model. The antiresonance condition is then derived in Sec. III. Two calculations for more realistic systems are presented in Sec. IV. We then conclude with Sec. V. The Appendix summarises the calculation of the Green’s function for the semi-infinite 1D leads and takes the non-orthogonality of atomic orbitals into account.

## II. ANALYTIC THEORY: CHANGING HILBERT SPACES AND SOLUTION OF THE LIPPMANN-SCHWINGER EQUATION

Most theoretical studies of molecular wires have used tight binding bases of atomic orbitals for the molecular and lead Hamiltonians. The atomic orbitals on different atoms are not orthogonal to each other and, as we will show below, this non-orthogonality can have important physical consequences for molecular wire antiresonances. We treat this lack of orthogonality exactly in our analytic Lippmann-Schwinger (LS) theory<sup>26</sup> of antiresonances

in a molecule connected to single-channel leads by solving the problem in a new Hilbert space spanned by an orthogonal basis where we define a new energy-dependent Hamiltonian matrix.<sup>15</sup> We begin with a derivation and discussion of this change of Hilbert space which will be vital to our definition of a LS equation below.

We start with Schrödinger's equation for the eigenvectors  $\{|\Psi\rangle\}$  of a Hamiltonian  $H$ ,

$$H|\Psi\rangle = E|\Psi\rangle. \quad (1)$$

We wish to solve Eq.(1) for  $|\Psi\rangle$ . We begin by expressing  $|\Psi\rangle$  in a non-orthogonal basis  $\{|n\rangle\}$  of the usual physical Hilbert space  $A$  for the system as  $|\Psi\rangle = \sum_n \Psi_n |n\rangle$ . Inserting this expression for  $|\Psi\rangle$  into Eq.(1) and applying  $\langle m|$  we obtain

$$\sum_n H_{m,n} \Psi_n = E \sum_n S_{m,n} \Psi_n \quad (2)$$

where we define  $H_{m,n} = \langle m|H|n\rangle$  to be the Hamiltonian matrix and  $S_{m,n} = \langle m|n\rangle$  to be the overlap matrix. We note that if the basis  $\{|n\rangle\}$  is incomplete then Eq. (2) becomes an approximation that may be justified variationally.<sup>25</sup> In either case, we will assume that Eq.(2) provides an adequate description of the system of interest and our objective will be to solve it exactly for the coefficients  $\Psi_n$ .

We will assume in the following that the sums in Eq.(2) (and similar summations in the remainder of this article) converge absolutely<sup>27</sup> so that the order in which the summations are performed is unimportant. This assumption is justified for the physical applications that we will be considering where the non-orthogonal basis states  $\{|n\rangle\}$  will be atomic tight binding orbitals (or molecular orbitals confined to finite molecular segments) and only a finite number of these orbitals are considered on any particular site. For such basis states  $H_{m,n}$  and  $S_{m,n}$  decrease *exponentially* as the spatial separation between the tight binding sites associated with basis states  $|m\rangle$  and  $|n\rangle$  becomes large. This guarantees the absolute convergence of the summations in Eq.(2) even if the system is infinite in extent and  $|\Psi\rangle$  is a physical scattering state that extends throughout the system.

The absolute convergence of the series in Eq.(2) enables us to rewrite Eq.(2) as

$$\sum_n H_{m,n}^E \Psi_n = E \Psi_m \quad (3)$$

where

$$H_{m,n}^E = H_{m,n} - E(S_{m,n} - \delta_{m,n}). \quad (4)$$

We are concerned with open systems that have a continuous spectrum of energy eigenvalues. Thus our objective is to find the coefficients  $\Psi_n$  that satisfy Eq. (3) for every value of  $E$  belonging to the continuum of energy eigenvalues of the Hamiltonian  $H$ . To do this we find it convenient to consider the related matrix eigenproblem

$$\sum_n H_{m,n}^E \Psi'_n = E' \Psi'_m \quad (5)$$

where  $E'$  is any eigenvalue of the matrix  $H_{m,n}^E$  and the set of coefficients  $\{\Psi'_m\}$  form the corresponding eigenvector. The solution  $\{\Psi_m\}$  of Eq. (3) that we seek is then identical to

an eigenvector  $\{\Psi'_m\}$  of the matrix  $H_{m,n}^E$  for which the eigenvalue  $E'$  in Eq. (5) is equal to  $E$ .

We now re-interpret Eq. (5) as the matrix form of a new Schrödinger equation

$$H^E|\Psi\rangle' = E'|\Psi\rangle'. \quad (6)$$

involving a new Hamiltonian operator  $H^E$  and its eigenvectors  $|\Psi\rangle'$  in a new Hilbert space  $A'$ . We construct this new Hilbert space as follows: We first form the vector space  $V'$  that is spanned by an *orthonormal* basis (that we denote  $\{|n\rangle'\}$ ) of the matrix  $H_{m,n}^E$ .<sup>28</sup> [Note that the basis vectors  $|n\rangle'$  defined in this way are abstract mathematical entities which should not be confused with the (non-orthogonal) physical state vectors  $|n\rangle$  of the original (physical) Hilbert space  $A$  or with any other vectors in that Hilbert space.] For the systems of interest in this work  $V'$  is infinite-dimensional and we define the Hilbert space  $A'$  to be the completion of  $V'$  with respect to the norm topology.<sup>29</sup> Eq. (5) will be the matrix form of Eq. (6) in Hilbert space  $A'$  as desired provided that the new Hamiltonian operator  $H^E$  is chosen so that its matrix elements satisfy  $\langle m'|H^E|n\rangle' = H_{m,n}^E$  and  $|\Psi\rangle' = \sum_n \Psi'_n|n\rangle'$ . It follows from Eq.(4) that the operator  $H^E$  is Hermitian in  $A'$  because  $E$  is real and  $H_{m,n}$ ,  $S_{m,n}$  and  $\delta_{m,n}$  are Hermitian matrices.

Thus we have transformed a problem that was formulated in terms of a non-orthogonal basis into an equivalent one in an orthogonal basis of a *different* Hilbert space. Essentially what we have done is to create a new problem (which may be easier to solve) from our old one. This is quite different from other orthogonalisation schemes (such as that of Gramm-Schmidt or Löwdin<sup>25</sup>). In those schemes the original non-orthogonal basis of the Hilbert space is orthogonalised by transforming it into a new orthogonal basis of the same space. Our method has no such orthogonalisation procedure: instead we assume our new operators and eigenvectors to be expressed in terms of an orthogonal basis of a new space and define them so that the matrix eigenvalue problem, Eq. (5) follows. This re-definition creates an energy dependent Hamiltonian whose energy dependence will be important in our discussion of antiresonances below.

It should be noted that only the eigenvectors of  $H^E$  that have the eigenvalue  $E$  have the same coefficients  $\Psi_n$  as eigenvectors of the true Hamiltonian  $H$ . The other eigenvectors of  $H^E$  do not correspond to any eigenstate of the physical Hamiltonian  $H$ , but they never the less play an important role when calculating the Green's function corresponding to  $H^E$  which appears in the Lippmann-Schwinger equation below.

Since no assumptions (other than the absolute convergence of the summations in Eq.(2)) have been made about the nature of the system being considered, this method of orthogonalisation by switching to a new Hilbert space is extremely general. If the basis states  $\{|n\rangle\}$  are tight binding atomic orbitals then the present transformation (unlike the transformation to Wannier functions) can be used irrespective of the types of atoms involved or their locations in space. Furthermore, our transformation has the additional flexibility that the non-orthogonal basis states need not all be of the same generic type. For example, some of them may be atomic orbitals and others molecular orbitals on some cluster(s) of atoms that form a part of the physical system. This flexibility will be exploited below. We now proceed to outline the application to antiresonances in molecular wires.

Our analytic theory for electron transport in molecular wires is based on an idealised model consisting of a molecule connected to two identical single-channel ideal leads which

are represented by 1D chains of atoms (shown in Fig. 1). We solve for the scattering wavefunction  $|\Psi\rangle$  which describes an electron incident from the left lead with energy  $E$  and having a probability  $T(E)$  to scatter through the molecule to the right lead. The system satisfies  $H|\Psi\rangle = E|\Psi\rangle$ , where  $H = H_0 + W$ .  $H_0$  is the Hamiltonian for the three isolated systems consisting of the two leads and the molecule and  $W$  couples the lead sites adjacent to the molecule with the sites on the molecule.

We now introduce a non-orthogonal basis consisting of atomic orbitals  $\{|n\rangle\}$  with  $n = -\infty, \dots, -1$  on the left lead and  $n = 1, \dots, \infty$  on the right lead and a set of molecular orbitals (MO's)  $\{|\phi_j\rangle\}$  for the molecule. In this basis the wavefunction has the form,

$$|\Psi\rangle = \sum_{n=-\infty}^{-1} \Psi_n |n\rangle + \sum_{n=1}^{\infty} \Psi_n |n\rangle + \sum_j c_j |\phi_j\rangle \quad (7)$$

The transmission probability  $T$  is found from  $|\Psi\rangle$  by utilising the boundary conditions that the wavefunction satisfies. On the left lead the wavefunction consists of a rightward propagating Bloch wave along with a reflected leftward propagating Bloch wave. This can be written as  $|\Psi_L\rangle = \sum_{n=-\infty}^{-1} (\exp(iny) + r \exp(-iny)) |n\rangle$ , where  $r$  is the reflection coefficient. The right lead is identical to the left lead and on it the wavefunction has the form of a transmitted Bloch wave  $|\Psi_R\rangle = \sum_{n=1}^{\infty} t \exp(iyn) |n\rangle$  where  $t$  is the transmission coefficient. Thus the transmission probability that enters the Landauer electrical conductance of the wire is given by  $T = |t|^2 = |\Psi_1|^2$ . The electron's velocity is the same on both leads and so the ratio of velocities that normally appears in the formula for  $T$  is equal to unity.

In the non-orthogonal basis solving for  $\Psi_1$  analytically is difficult thus we change to the new Hilbert space where the solution is more straightforward. The transmission probability  $T$  is unaffected since the coefficient  $\Psi'_1$  remains the same for fixed  $E$ . The new Hamiltonian operator  $H^E$  and its eigenvectors  $\{|\Psi'\rangle\}$  are now assumed to be expressed in an orthonormal basis  $\{|n'\rangle, |\phi_j'\rangle\}$  with the new Hamiltonian matrix elements defined in terms of the matrix elements of the initial Hamiltonian  $H$  and the overlap matrix  $S$  via Eq. (4). Thus if there is any non-orthogonality in the original basis sets of the three isolated systems then  $H_0$  becomes  $H_0^E$ . The non-orthogonality between the orbitals on the molecule and the leads changes  $W$  to  $W^E$ .

We evaluate  $\Psi'_1$  by solving a Lippmann-Schwinger (LS) equation. This equation is defined only after the transformation and is given by,

$$|\Psi'\rangle = |\Phi_o'\rangle + G_o(E) W^E |\Psi'\rangle. \quad (8)$$

Here  $G_o(E) = (E - H_0^E)^{-1}$  is the Green's function for the decoupled system of left, right leads and the molecule. The electron is initially in the eigenstate  $|\Phi_o'\rangle$  of the left lead propagating with an energy  $E$ . It is confined to the left lead and is written as

$$|\Phi_o'\rangle = \sum_{n=-\infty}^{-1} (\Phi'_o)_n |n'\rangle. \quad (9)$$

It should be emphasised that the LS equation Eq. (8) is only valid after the change to the new Hilbert space where the basis is orthogonal. This is because it is now possible to distinctly separate the states on the leads from those on the molecule. The original

non-orthogonal basis did not allow for this clear distinction and contradictions arise if the analogs of the entities in Eq. (8) are constructed using this basis.

The free propagator,  $G_o$ , can be expressed in terms of the energy eigenstates of  $H_0^E$  of the isolated leads and of the molecule. It will be written as a sum of three separate free propagators for the left and right leads and the molecule,  $G_o^L$ ,  $G_o^R$ , and  $G_o^M$  respectively. The left and right leads have been assumed to be identical so their free propagators will be the same. For the leads with energy eigenstates  $\{|\Phi_o(y)\rangle'\}$  having energy  $\epsilon(y)$

$$G_o^R = \sum_y \frac{|\Phi_o(y)\rangle'\langle\Phi_o(y)|'}{E - \epsilon(y)} \quad (10)$$

Here  $y$  is the wave number in units of the inverse lattice parameter. Expressing the eigenstates in terms of the basis,  $\{|n\rangle'\}$ , the free propagator on the leads has the form,

$$G_o^R = \sum_{n=1}^{\infty} \sum_{m=1}^{\infty} (G_o^R)_{n,m} |n\rangle'\langle m|' \quad (11)$$

The matrix elements,  $(G_o^R)_{n,m}$  are evaluated analytically in the Appendix.

For the molecule the free propagator expressed in terms of its MO's is

$$G_o^M = \sum_j \frac{|\phi_j\rangle\langle\phi_j|}{E - \epsilon_j} = \sum_j (G_o^M)_j |\phi_j\rangle\langle\phi_j| \quad (12)$$

Using these expressions for the wavefunctions and the free propagator the LS equation becomes (the ' have been dropped)

$$\begin{aligned} & \sum_{n=-\infty}^{-1} \Psi_n |n\rangle + \sum_{n=1}^{\infty} \Psi_n |n\rangle + \sum_j c_j |\phi_j\rangle = \sum_{n=-\infty}^{-1} (\Phi_o)_n |n\rangle + \\ & \left( \sum_{n,m=-\infty}^{-1} (G_o^L)_{n,m} |n\rangle\langle m| + \sum_{n,m=1}^{\infty} (G_o^R)_{n,m} |n\rangle\langle m| + \sum_j (G_o^M)_j |\phi_j\rangle\langle\phi_j| \right) W^E \times \\ & \left( \sum_{n=-\infty}^{-1} \Psi_n |n\rangle + \sum_{n=1}^{\infty} \Psi_n |n\rangle + \sum_j c_j |\phi_j\rangle \right) \end{aligned}$$

We now apply the bras  $\langle -1|$ ,  $\langle\phi_j|$ , and  $\langle 1|$  to the above equation, making use of their formal mutual orthogonality. This gives the following set of simultaneous linear equations

$$\Psi_{-1} = (\Phi_o)_{-1} + (G_o^L)_{-1,-1} \sum_j \langle -1|W^E|\phi_j\rangle c_j \quad (13)$$

$$c_j = (G_o^M)_j (\langle\phi_j|W^E|-1\rangle \Psi_{-1} + \langle\phi_j|W^E|1\rangle \Psi_1) \quad (14)$$

$$\Psi_1 = (G_o^R)_{1,1} \sum_j \langle 1|W^E|\phi_j\rangle c_j \quad (15)$$

where

$$\langle 1|W^E|\phi_j\rangle = W_{1,j}^E = W_{1,j} - ES_{1,j} \quad (16)$$

which is the interaction matrix element between the the lead orbital adjacent to the molecule and the  $j^{th}$  MO. Notice it includes the overlap between the  $j^{th}$  MO and the first lead orbital.

These equations can be solved for the unknowns,  $\Psi_{-1}$ ,  $\Psi_1$ , and the  $c_j$ , yielding

$$\Psi_1 = \frac{A(\Phi_o)_{-1}}{[(1-B)(1-C)-AD]} \quad (17)$$

$$\Psi_{-1} = \frac{(1-B)(\Phi_o)_{-1}}{[(1-B)(1-C)-AD]} \quad (18)$$

$$c_j = (G_o^M)_j \left( \frac{W_{j,1}^E A + W_{j,-1}^E (1-B)}{[(1-B)(1-C)-AD]} \right) (\Phi_o)_{-1} \quad (19)$$

where, making use of the symmetry between  $G_o^L$  and  $G_o^R$ ,

$$\begin{aligned} A &= (G_o^R)_{1,1} \sum_j W_{1,j}^E (G_o^M)_j W_{j,-1}^E \\ B &= (G_o^R)_{1,1} \sum_j (W_{1,j}^E)^2 (G_o^M)_j \\ C &= (G_o^R)_{1,1} \sum_j (W_{-1,j}^E)^2 (G_o^M)_j \\ D &= (G_o^R)_{1,1} \sum_j W_{-1,j}^E (G_o^M)_j W_{j,1}^E \end{aligned}$$

The transmission probability  $T(E)$  is given by  $|\Psi_1|^2$ .

### III. ANTIRESONANCE CONDITION AND MECHANISMS

An antiresonance is defined to be a zero of the electron transmission probability. Since  $T(E)$  is given by the squared modulus of  $\Psi_1$ , the zeroes occur where  $\Psi_1$  is zero. From Eq. (17) this happens when  $A = 0$ . Thus the antiresonance condition is

$$(G_o^R)_{1,1} \sum_j W_{1,j}^E (G_o^M)_j W_{j,-1}^E = 0 \quad (20)$$

or

$$\sum_j \frac{(W_{1,j} - ES_{1,j})(W_{j,-1} - ES_{j,-1})}{E - \epsilon_j} = 0 \quad (21)$$

where the sum over  $j$  includes just the MO's.

The antiresonance conditions (20) and (21) that we have derived allows us to identify two distinct mechanisms that can give rise to antiresonances in molecular wire transport.

In the first of these mechanisms, antiresonances arise due to an interference between the different MO's of the molecule. This is seen directly from Eq. (21): An electron incident from the left lead, hops from the lead site adjacent to the molecule onto each of the molecular orbitals with a weight  $W_{j,-1}^E$ . It then propagates through each of the different orbitals  $j$ . These processes interfere with each other as the electron propagates through the molecule and proceeds to hop onto the first lead site on the right lead with a weight  $W_{1,j}^E$ .



What is particularly interesting about this molecular mechanism and differentiates it qualitatively from a standard multi-beam interference problem encountered in optics via a diffraction grating, is that the antiresonances arise from *interference between molecular states that differ in energy*. It is also not possible to make an analogy between this effect and Fano resonances<sup>30</sup>, which are a good analog of the antiresonances in electron waveguides of the stub-tuner type<sup>21</sup>. For those waveguides, the antiresonances arise from interference between the direct transmission of a continuum of electron modes (which exists in the semiconductor quantum wire) and transmission via discrete modes that reside within the resonator. In our model, transmitted electrons *must* pass through the molecule so that there is no *direct* transmission of continuum modes from the left to the right lead and the Fano mechanism does not apply. The molecular wire antiresonances are also not analogous to those found in the Fabry-Perot model of double barrier resonant tunneling<sup>23</sup>. In that model, electrons couple to different modes within the well which interfere upon exiting the well. But these modes are all at the same energy. As was mentioned above, the interfering molecular states are at different energies.

This antiresonance mechanism is qualitatively similar to that which was found in previous work on electron transfer between donors and acceptors in molecules,<sup>12</sup> however the antiresonance conditions (20) and (21) that we have derived differ from those that were obtained earlier partly because the non-orthogonality of the atomic orbitals has been included in our theory. In particular, for a molecule with  $N$  distinct energy levels, the resonance condition (21) gives rise to a polynomial equation of degree  $m = (N - 1) + 2$ , so there can be at most  $m$  antiresonances for this model. Neglecting the overlaps  $S_{1,j}$  and  $S_{j,-1}$  between atomic orbitals on different atoms leads to a polynomial equation of a lower order and can yield qualitatively different predictions, as will be made clear below.

The second antiresonance mechanism that we identify on the basis of the conditions (20) and (21) has no analog in previous work and is at first sight quite surprising since it is due entirely to the non-orthogonality of atomic orbitals on different atoms. It occurs when only a single molecular orbital  $a$  couples appreciably to the leads, which should happen in some real systems for reasons of symmetry, as is discussed in the next section. In such cases Eq. (21) becomes  $(W_{a,-1} - ES_{a,-1})(W_{1,a} - ES_{1,a}) = 0$ . As many as two antiresonances are possible in this case. They arise because the energy dependent coupling is equal to zero between the leads and the molecule at the energies  $E$  for which the energy dependent hopping parameter  $(W_{a,-1} - ES_{a,-1})$  or  $(W_{1,a} - ES_{1,a})$  vanishes. This cancellation arises because of the non-orthogonality between the atomic orbitals of the molecule and those of the leads.

We explore some specific molecular systems that should exhibit each of the above antiresonance mechanisms in the following section.

The present theory is readily extended to include second and more distant neighbour interactions and overlaps. These will act as a perturbations to the antiresonance values. If the interactions are sufficiently long ranged so as to couple the two leads to each other directly in addition to coupling them indirectly via the molecule, other antiresonance mechanisms, including Fano-like effects become possible. However detailed consideration of these is beyond the scope of this paper.

#### IV. MULTICHANNEL LEADS AND METALLIC CONTACTS

The above model has yielded an equation which predicts energies at which antiresonances should occur in molecular wire systems. It was based on a highly idealised model which assumed that there was only a single propagating electronic mode in the leads. This single mode was only allowed to interact with the molecular orbitals on the molecule. Real leads, whether organic or inorganic, will certainly not be as simple. However the two calculations presented below show that the key predictions made by this simple model should apply quantitatively to some more complex systems as well.

A good approximation to a 1D lead with only one orbital per site is conjugated trans-polyacetylene. The  $\pi$  backbone of this polymer is orthogonal to the  $\sigma$  orbitals in the plane. Second nearest neighbour  $\pi$  interactions between carbon atoms are also small compared to nearest neighbour interactions. The conjugation of the polymer creates a band gap in the  $\pi$  energy band of this system. If one inserts a molecule whose spectrum also consists of  $\pi$  and  $\sigma$  molecular orbitals into the backbone of this structure in a suitably symmetric way, only the  $\pi$  band of the polymer will interact with the  $\pi$  states of the molecule. It is important however that the inserted molecule be long enough so that the  $\pi$  orbitals on the left polyacetylene lead can not overlap with the  $\pi$  orbitals on the right lead. Otherwise electrons could hop directly from the left lead to the right lead without passing through the inserted molecule. Thus our simple model is applicable to a system consisting of  $\pi$  conjugated leads attached to a molecular wire with  $\pi$  states if the wire is long enough that there is no direct interaction between the leads and the geometry is such that  $\sigma$  -  $\pi$  hybridization between the leads and molecular wire is forbidden. The antiresonance condition Eq. (21) should be able to predict the antiresonances of these more complicated systems if the energies  $\epsilon_j$  of the  $\pi$  molecular orbitals are specified along with their interaction energies  $W_{j,1}$  and  $W_{-1,j}$  with the  $\pi$  mode of the leads and the corresponding orbital overlaps  $S_{j,1}$  and  $S_{-1,j}$ .

We now proceed to calculate the electron transmission probability for two such model systems. Our calculations are based on a numerical method which determines the transmission probability of a molecular wire coupled to multichannel tight-binding leads.<sup>10,31</sup> The multichannel leads are constructed out of multi-atom unit cells which are then attached to the molecular wire. The non-orthogonality within the leads and the molecule and also between the leads and the molecule is treated with the use of our transformation. The calculation proceeds by evaluating the band structure of the left and right leads from which it is then possible to determine the propagating electron modes (Bloch states)  $\{|\Phi_j^+\rangle, |\Phi_j^-\rangle\}$  at a given energy  $E$ . In these multichannel calculations the wavefunction for an electron incident in the  $i^{th}$  mode has the following boundary conditions. In the left lead,  $|\Psi_L^i\rangle = |\Phi_i^+\rangle + \sum_j r_{j,i} |\Phi_j^-\rangle$ . On the molecule the wavefunction is a linear combination of the atomic orbitals on the molecule. On the right lead the wavefunction is  $|\Psi_R^i\rangle = \sum_j t_{j,i} |\Phi_j^+\rangle$ . With the above form for the wavefunction we then solve Schrödinger's equation  $H|\Psi^i\rangle = E|\Psi^i\rangle$  for the molecular wire system to find the transmission amplitudes  $t_{j,i}$  which connect the modes  $i$  in the left lead to those in the right lead,  $j$ . The transmission probability is then found using

$$T(E) = \sum_i \sum_j \left| \frac{v_i}{v_j} \right| |t_{i,j}|^2 \quad (22)$$

where the sum over  $j$  is over the rightward propagating modes in the left lead and the sum

over  $i$  is over rightward propagating modes in the right lead. The velocity ratio now appears since the velocities of modes in the left and right leads may be different. We now show that provided the model system meets the assumptions of the analytical model presented above, this more sophisticated numerical method yields results consistent with the analytical predictions.

The first calculation utilises the trans-polyacetylene polymer to model the left and right ideal leads. We have calculated the band structure for these leads and this is shown in Fig. 2. The unit cell for the polyacetylene lead was taken to consist of two CH groups and the group spacing was taken from Su *et al*<sup>32</sup>. The  $\pi$  band extends from around -14.5 eV to -5 eV and has a band gap of around -1.4 eV starting at -11.2 eV. The upper  $\pi$  band is unoccupied. The other energy bands are  $\sigma$  modes. In reality, it is well known from electron transport studies of trans-polyacetylene that soliton and polaron formation is favoured when charge is injected into the chain.<sup>32,33</sup> We do not include such effects in the present calculation; here the infinite polyacetylene chains are taken to be static periodic structures, they represent ideal quasi-one dimensional leads. For this system we consider a molecular wire with three  $\sigma$  states but with just a single  $\pi$  level to which the leads couple. The model parameters for the molecular wire's coupling of its  $\pi$  state to the  $\pi$  band of the leads are chosen so that our analytic antiresonance condition (21) predicts an antiresonance in the occupied  $\pi$  energy band and at an energy where only a  $\pi$  mode propagates in the left lead. If there were a transmitted  $\sigma$  mode present at the energy of the antiresonance as well its transmission would be superimposed on the  $\pi$  transmission which would possibly obscure the antiresonance. A single  $\pi$  mode propagates through this system between the energies of -12 eV and -11.2 eV. For our molecule with a single  $\pi$  state the antiresonance arising out of the interaction with the left lead is predicted by (21) to occur at an energy of  $E = W_{\pi,-1}/S_{\pi,-1}$ . If we choose the overlap to be 0.3 and an interaction energy of -3.525 eV between the  $\pi$  state of the molecule and the  $\pi$  orbital on the nearest carbon atom on the lead, the antiresonance is predicted to occur at -11.75 eV. Since the interaction energy is related to the overlap the two are not completely arbitrary, however the interaction energy also depends on the energy of the molecular orbital which in principle could be chosen to yield the above coupling energy. The numerically calculated electron transmission probability for this system is shown by the solid line in Fig. 3. The antiresonance is clearly seen at -11.75 eV. There is also a sharp drop off in transmission at -12 eV where there are no longer any  $\sigma$  modes incident from the left lead. Also shown (the dashed line in Fig. 3) is the result of the analytic calculation using the (LS) equation above. This was done for a single mode lead with its energy band spanning the width of the polyacetylene  $\pi$  band. The couplings and overlaps were chosen to be the same as those used in the multi-mode case. The agreement between the two calculations is quite good in the vicinity of the antiresonance.

The above calculation was for infinite polyacetylene leads which are known to be insulators. Thus performing a conductance experiment on such a system would be impossible. Recent experiments on molecular wires have used metallic nanocontacts connected to the molecule<sup>2</sup>. The system that we base our next calculation on is such a mechanically controlled break junction (MCBJ) which is bridged by a single molecule. The metallic contacts will be taken to be gold. We consider the molecular wire to consist of left and right  $\pi$  conjugated chain molecules attached to what we will call the “active” molecule. The purpose of these conjugated chains is to act as a filter to the many modes that will be incident from the

metallic leads. For appropriate energies they will restrict the propagating electron mode to be only  $\pi$  like. The electronic structure of the active molecule will be assumed to consist of  $\pi$  and  $\sigma$  like molecular orbitals. The  $\pi$  backbone of the chain molecules will only interact with the  $\pi$  orbitals of the active molecule and so our antiresonance condition should still be applicable in this model.

The multi-channel gold leads for our calculation are created using a unit cell composed of two layers of gold atoms in the (111) direction. Both layers have 20 gold atoms. Since the Fermi energy for gold resides in the 6s band we only use 6s orbitals on our gold atoms. The chain molecules consist of eight CH groups each. An atomic diagram of our system is shown in Fig. 4. The chain molecules are bonded to clusters consisting of 10 gold atoms that form the tips of the leads. The carbon atom nearest to the gold tip binds over the triangle of gold atoms with a perpendicular distance of 1.6 Angstroms. This larger molecular segment consisting of the gold tips, chain and active molecules is then attached to the left and right unit cells of the multichannel gold leads. The chains are now finite polyacetylene and so they now have discrete energy states rather than bands, the molecular states on these chains are  $\pi$  like for energies in the polyacetylene  $\pi$  band. This gives rise to the filtering process mentioned above. The active molecule is chosen to have two  $\sigma$  states and two  $\pi$  states. Unlike the infinite leads in the preceding calculation the finite chain molecules will conduct. Their  $\pi$  like orbitals will only couple to the two  $\pi$  states of the active molecule.

The Fermi energy for our gold leads is around -10 eV which lies within the  $\pi$  band. Thus we would like an antiresonance to occur somewhere near this energy. Again, for this model system, we make some ad-hoc choices for our parameters. The two active molecular  $\pi$  states are chosen to have energies  $\epsilon_a = -14.0$  eV and  $\epsilon_b = -11.0$  eV. The interactions between these states and the  $\pi$  orbitals on the carbon atoms directly adjacent to the active molecule are  $W_{a,-1} = W_{1,a} = -3.0$  eV, and  $W_{b,-1} = -W_{1,b} = 1.25$  eV. The overlaps are  $S_{a,-1} = S_{1,a} = 0.14$  and  $S_{b,-1} = -S_{1,b} = -0.2$ . Solving the cubic equation to which Eq. (21) reduces in this case, yields three real energies, one of them in the desired energy range predicting an antiresonance at -10.08 eV. We now proceed to calculate the electronic transmission through this system.

Recent work has studied electron transport through finite conjugated chains attached to metallic leads with the inclusion of inelastic degrees of freedom.<sup>34</sup> In that study it was shown that electron injection onto the chains induces a small polaron defect. However, for chains of small enough length (10 CH groups or less) it was found that this polaron defect did not have an appreciable effect on the electron transport compared to the static case. To see how atomic positional disorder on the chains affects the antiresonance, we have numerically calculated the transmission probability for several different static atomic configurations of the finite poly-acetylene chains and these are shown in Fig. 5a. The solid curve corresponds to dimerized trans-polyacetylene. The short-dashed curve corresponds to an undimerized chain. The long-dashed curve corresponds to chains with a static soliton. In all three curves the antiresonance is present, although the magnitude varies in the regions outside of the antiresonance. Although dynamic effects of polaron or soliton formation have not been included in the present study, we have shown that the existence of the antiresonance is not affected by the disorder on the conjugated chains or by whether or not they dimerize. Based on the results presented in Ref.<sup>34</sup> for short conjugated chains, we expect that the antiresonance would still survive even with the inclusion of dynamical effects where the

couplings and overlaps may vary.

In experiments on molecular wires the electric current  $I$  through the molecule is measured as a function of voltage  $V$ . The differential conductance is then determined by taking the derivative  $G = dI/dV$ . We calculate this differential conductance by using a generalisation of the Landauer formula which relates the electric current to the transmission probability  $T(E)$  that is given by Eq. (22). The finite voltage, finite temperature Landauer formula that we use is

$$I(V) = \frac{2e}{h} \int_{-\infty}^{\infty} dE T(E) \left( \frac{1}{\exp[(E - \mu_s)/kT] + 1} - \frac{1}{\exp[(E - \mu_d)/kT] + 1} \right) \quad (23)$$

where  $\mu_s = \epsilon_f + eV/2$  and  $\mu_d = \epsilon_f - eV/2$  and where  $\epsilon_f$  is the common Fermi energy of the leads and  $V$  is the applied bias voltage.

The differential conductance at room temperature,  $T = 293$  K calculated from the above current for two different choices of Fermi energy is shown in Fig. 5b. (It was calculated using the transmission probability for the dimerized chain). The solid curve corresponds to a choice of Fermi energy of -10.2 eV. Because it lies to the left of the antiresonance in a region of strong transmission the conductance is strong at 0 V. It then drops at around 0.2 V when the antiresonance is crossed. The dashed curve was calculated using a Fermi energy of -10.0 eV. It starts in a region of lower transmission and thus the antiresonance suppresses the increase in current. After 0.2 V the large transmission to the left of the antiresonance is sampled and the current rises sharply. So in both cases the antiresonance has served the roll of lowering the conductance. It is conceivable to think of utilising more antiresonances in a narrow energy range to create a more observable conductance drop. It should also be pointed out that the differential conductance was calculated using the electron transmission evaluated at 0 V. If one assumes a linear voltage drop between the leads this approximation is reasonably valid since the “active” molecule is located roughly in the middle of the bridge between the two leads and the site energies will not be shifted much by the applied field. The coupling elements are assumed not to shift in the applied field. With these assumptions, the roots of the antiresonance condition do not change significantly and so the location of the antiresonance at -10.08 eV does not shift appreciably.

## V. CONCLUSIONS

In this article we have presented a theoretical study that suggests that antiresonance phenomena should be observable in the electrical conductance of molecular wires connected to metallic nano-contacts. We solved analytically a simple model that exhibits antiresonances and incorporates for the first time the effects of the non-orthogonality of tight binding atomic orbitals on different atoms, an important feature of all molecular systems. The non-orthogonality was treated exactly by defining a new energy dependent Hamiltonian operator and corresponding eigenvector, and then expressing them in an orthonormal basis of a new Hilbert space. This method was both simple and very general and should be useful for treating a wide variety of problems which are best defined in a non-orthogonal basis. The Lippmann-Schwinger equation for the transmission through the molecular wire was solved in this new representation and an analytic description of the antiresonances was obtained.

In our model the molecular antiresonances occur due to two different mechanisms. One of these is interference between the contributions of different molecular orbitals as the electron propagates through the molecule. The other is the vanishing of the effective hopping matrix element between a pair of atomic orbitals that is due to the non-orthogonality of those orbitals. In both cases taking the non-orthogonality into account exactly is necessary to obtain reliable results. The antiresonance condition that we derive and that determines the energies where the transmission is zero, only depends on the molecular Green's function and on the energy dependent interaction energies of the molecular states with the leads.

We have shown that this simple analytically solvable model has predictive power for more complex systems by performing detailed numerical calculations. The first of these calculations was for a system on which conductance measurements are not feasible because of the insulating nature of the leads. However it demonstrated how a molecular wire with a single  $\pi$  state can generate a transmission antiresonance due to the cancellation of the effective coupling between the lead and the molecule as a consequence of the mutual non-orthogonality of atomic orbitals. The second calculation was for a system in which molecular antiresonances should in principle be accessible to experiment: a molecular wire bridging a break junction between two gold nanocontacts. In it we have suggested the use of  $\pi$  conjugated chains to act as mode filters. The use of these filters could be useful in most molecular wire systems where limiting the number of propagating modes to just one would be advantageous. For filters connected to an "active" molecule it is possible to create an antiresonance near the Fermi energy of the metal contacts. The antiresonance was predicted to manifest itself by producing a drop in the differential conductance. In both cases the location of the antiresonance found in the numerical simulations was in agreement with the prediction of our simple analytic model.

We thank R. Akis for helpful correspondence regarding antiresonances in semiconductor stub tuners. This work has been supported by NSERC.

## VI. APPENDIX: GREEN'S FUNCTION FOR IDEAL LEADS

The ideal 1D leads are treated using TBA, where the site energy is  $\alpha$ , and the nearest neighbour hopping energy is  $\beta$ . The overlap between nearest neighbour lead sites is  $\omega$  and is used to define an energy dependent hopping parameter  $\beta^E = \beta - E\omega$  for an electron with energy  $E$ . This allows us to use an effective orthonormal basis. The reduced wavevector,  $y$ , of a propagating electron can be found from the equation  $\epsilon(y) = \alpha + 2\beta^E \cos(y)$ . The leads are semi-infinite. Because of this the boundary conditions placed on the wavefunction are such that it is zero on site 0. Thus a valid choice for an incident electron state is a linear combination of a forward and backward propagating Bloch state, given by,

$$|\Phi_o(y)\rangle = \sum_{n=1}^{\infty} (\Phi_o(y))_n |n\rangle = \sum_{n=1}^{\infty} \frac{1}{\sqrt{2N}} (e^{iny} - e^{-iny}) |n\rangle \quad (24)$$

The matrix element for the free propagator of the lead between sites  $n$  and  $n'$  is given by,

$$(G_o^R)_{n,n'} = \sum_y \frac{(\Phi_o(y))_n (\Phi_o(y))_{n'}^*}{E - \epsilon(y) + i\delta} \quad (25)$$

Using the above expression for  $(\Phi_o(y))_n$ , the matrix element becomes,

$$(G_o(E))_{n,n'} = \frac{1}{2N} \sum_y \frac{e^{iy(n-n')} + e^{iy(n'-n)} - e^{iy(n+n')} - e^{iy(-n-n')}}{E - \epsilon(y) + i\delta} \quad (26)$$

As  $N$  becomes large the above summation goes over to an integral which is given by,

$$(G_o^R)_{n,n'} = \frac{1}{2Na} \frac{L}{2\pi} \int_{-\pi}^{\pi} \frac{e^{iy(n-n')} + e^{iy(n'-n)} - e^{iy(n+n')} - e^{iy(-n-n')}}{E - \epsilon(y) + i\delta} dy \quad (27)$$

where  $L = Na$  and  $a$  is the lattice parameter of the chain. Only the matrix element on the first site in the lead is needed, since this is the only site which is coupled to the molecule, so  $n$  and  $n'$  are set equal to 1. Substituting the expression for  $\epsilon(y)$ , the following integral is arrived at,

$$(G_o^R)_{1,1} = \frac{1}{8\pi\beta^E} \int_{-\pi}^{\pi} \frac{2(1 - e^{2iy})}{\frac{E-\alpha}{2\beta^E} + \frac{i\delta}{2\beta^E} - \cos y} dy \quad (28)$$

This integral can be evaluated by performing contour integration, and the result is,

$$(G_o^R)_{1,1} = \frac{1}{2\beta^E} \frac{(1 - e^{i2y_o})}{\sin y_o} \quad (29)$$

where  $y_o$  satisfies the condition  $\frac{(E-\alpha)}{2\beta^E} - \cos y_o = 0$ .

## REFERENCES

- <sup>1</sup> See, for example, *Proceedings of the Conference on Molecular Electronics: Science and Technology*, December 1997, Humacao, Puerto Rico, edited by A. Aviram, Ann. New York Academy of Science, June (1998).
- <sup>2</sup> M. A. Reed, C. Zhou, C. J. Muller, T. P. Burgin, and J. M. Tour, *Science* **278**, 252 (1997).  
C. Zhou, M. R. Deshpande, and M. A. Reed, *Appl. Phys. Lett.* **71**, 611 (1997).
- <sup>3</sup> S. Datta, W. Tian, S. Hong, R. Reifenberger, J. I. Henderson and C. P. Kubiak, *Phys. Rev. Lett.* **79**, 2530 (1997).
- <sup>4</sup> R. P. Andres, J. D. Bielefeld, J. I. Henderson, D. B. Janes, V. R. Kolagunta, C. P. Kubiak, W. J. Mahoney, and R. G. Osifchin, *Science* **273**, 1690 (1996).
- <sup>5</sup> L. A. Bumm, J. J. Arnold, M. T. Cygan, T. D. Dunbar, T. P. Burgin, L. Jones II, D. L. Allara, J. M. Tour, P. S. Weiss, *Science* **271**, 1705 (1996).
- <sup>6</sup> M. P. Samanta, W. Tian, S. Datta, J. I. Henderson, and C. P. Kubiak, *Phys. Rev. B* **53**, R7626 (1996).
- <sup>7</sup> M. Kemp, A. Roitberg, V. Mujica, T. Wanta and M. A. Ratner, *J. Phys. Chem* **100**, 8349 (1996).
- <sup>8</sup> C. Joachim, and J. F. Vinuesa, *Europhys. Lett.* **33**, 635 (1996).
- <sup>9</sup> V. Mujica, M. Kemp, A. Roitberg and M. Ratner, *J. Chem. Phys.* **104**, 7296 (1997).
- <sup>10</sup> E. Emberly and G. Kirczenow, *Ann. New York Academy of Science*, **852**, 54 (1998). E. Emberly and G. Kirczenow, *Phys. Rev. B*, **58**, 10911 (1998).
- <sup>11</sup> R. Landauer, *IBM J. Res. Dev.* **1**, 223 (1957); R. Landauer, *Phys. Lett.* **85A**, 91 (1981)
- <sup>12</sup> M. A. Ratner, *J. Phys. Chem.* **94**, 4877 (1990).
- <sup>13</sup> J. M. Lopez-Castillo, A. Filali-Mouhim, J. P. Jay-Gerin, *J. Phys. Chem.* **97**, 9266 (1993).
- <sup>14</sup> A. Cheong, A. E. Roitberg, V. Mujica, and M. A. Ratner, *J. Photochem. Photobiol. A: Chem.* **82**, 81 (1994).
- <sup>15</sup> A brief summary of some of the results has been published; E. Emberly and G. Kirczenow, *Phys. Rev. Lett.*, **81**, 5205 (1998).
- <sup>16</sup> F. Sols, M. Macucci, U. Ravaioli, and K. Hess, *Appl. Phys. Lett.* **54**, 350 (1989); *J. Appl. Phys.* **66**, 3892 (1989).
- <sup>17</sup> S. Datta, *Superlatt. Microstruct.* **6**, 83 (1989).
- <sup>18</sup> Z.-L. Ji and K.-F. Berggren, *Phys. Rev. B* **45**, 6652 (1992).
- <sup>19</sup> E. Tekman and P. F. Bagwell, *Phys. Rev. B*, **48**, 2553 (1993).
- <sup>20</sup> P. J. Price, *Phys. Rev. B* **48**, 17301 (1993).
- <sup>21</sup> Z. Shao, W. Porod, and C. S. Lent, *Phys. Rev. B* **49**, 7453 (1994).
- <sup>22</sup> R. Akis, P. Vasilopoulos, and P. Debray, *Phys. Rev. B* **52**, 2805 (1995).
- <sup>23</sup> T. B. Boykin, B. Pezeshki, and J. S. Harris, Jr., *Phys. Rev. B* **46**, 12769 (1992).
- <sup>24</sup> T. B. Boykin, J. P. A. van der Wagt, and J. S. Harris, Jr., *Phys. Rev. B* **43**, 4777 (1991).
- <sup>25</sup> P. O. Löwdin, *J. Chem. Phys.* **18**, 365 (1950).
- <sup>26</sup> Antiresonances in the electron transfer between donors and acceptors in molecules have also been studied using the LS approach<sup>12</sup> however the effects of the non-orthogonality of the tight binding basis that we consider here were not included in that work.
- <sup>27</sup> See, for example R. C. Buck, *Advanced Calculus*, sec. 5.3, McGraw-Hill, 1978.
- <sup>28</sup> The basis vectors  $|n\rangle'$  of the matrix  $H_{m,n}^E$  may be visualized as the abstract infinite column



vectors  $\begin{pmatrix} \vdots \\ 0 \\ 1 \\ 0 \\ \vdots \end{pmatrix}$  on which the matrix  $H_{m,n}^E$  acts. See, for example S. I. Grossman, *Linear*

*Algebra*, sec. 5.3, 4th ed., Saunders College Publishing, 1991.

<sup>29</sup> See, for example, L. E. Ballentine, *Quantum Mechanics*, pp. 16-17, 1st ed., Prentice Hall, 1990.

<sup>30</sup> U. Fano, Phys. Rev. **124**, 1866 (1961).

<sup>31</sup> In the present calculations, intra-cell and inter-cell atomic orbital overlap on the leads has not been set to zero. The overlap between the unit cell adjacent to the molecule and the molecule has also been taken into account, which is an extension of previous work.<sup>10</sup>

<sup>32</sup> W. P. Su, J. R. Schrieffer and A. J. Heeger, Phys. Rev. Lett. **49**, 1698 (1979).

<sup>33</sup> W. P. Su, J. R. Schrieffer and A. J. Heeger, Phys. Rev. B **22**, 2099 (1980).

<sup>34</sup> H. Ness and A. J. Fisher, Phys. Rev. Lett. **83**, 452 (1999).

# FIGURES

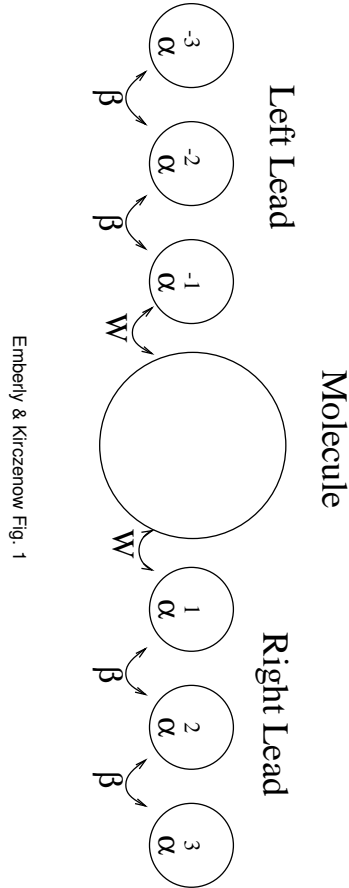
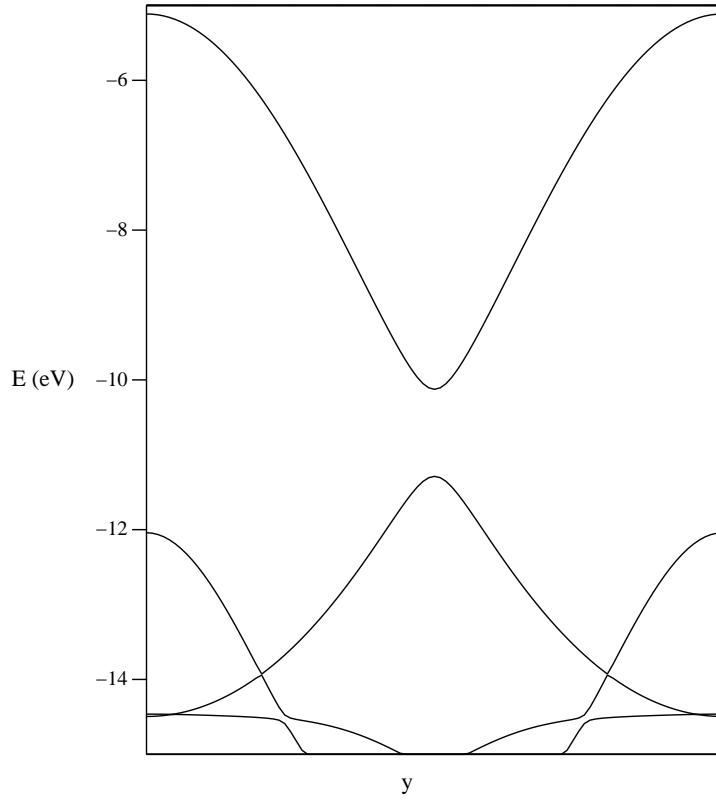
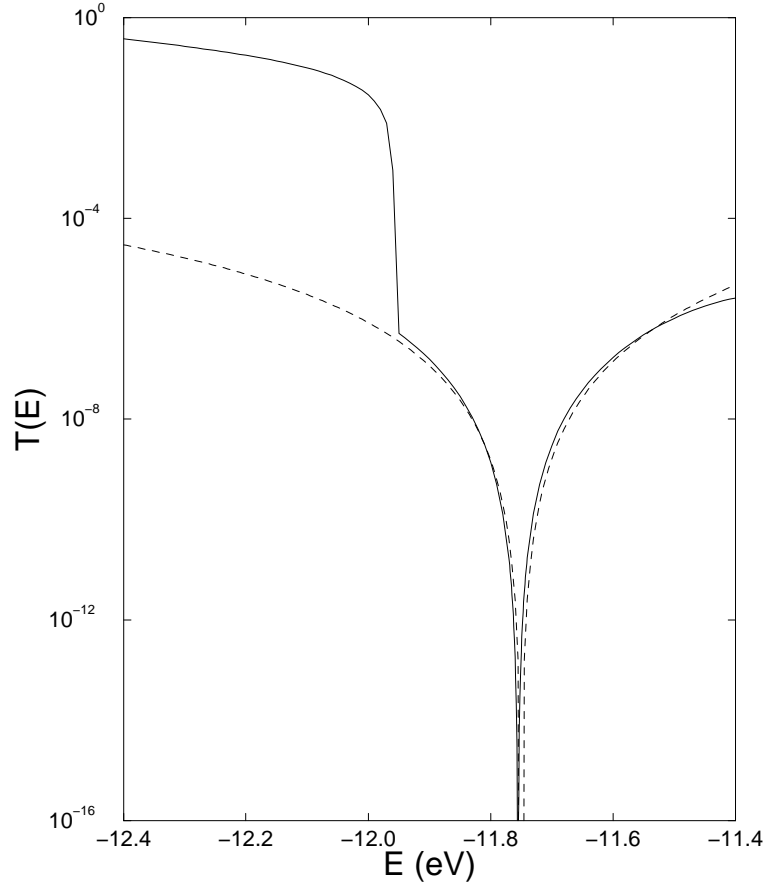


FIG. 1. A schematic diagram for the idealized model of a molecular wire, consisting of left and right single channel leads and the molecule. These three systems are described by the Hamiltonian  $H_0$ , with  $\langle n|H_0|n\rangle = \alpha$  and  $\langle n|H_0|m\rangle = \beta$  for  $n, m$  on the left or right leads with  $m = n \pm 1$ . On the molecule  $\langle \phi_j|H_0|\phi_k\rangle = \epsilon_j \delta_{j,k}$ . The molecular orbitals are coupled to the adjacent lead sites by  $W$ , with  $\langle -1|W|\phi_j\rangle = W_{-1,j}$  etc..



Emberly & Kirczenow Fig. 2

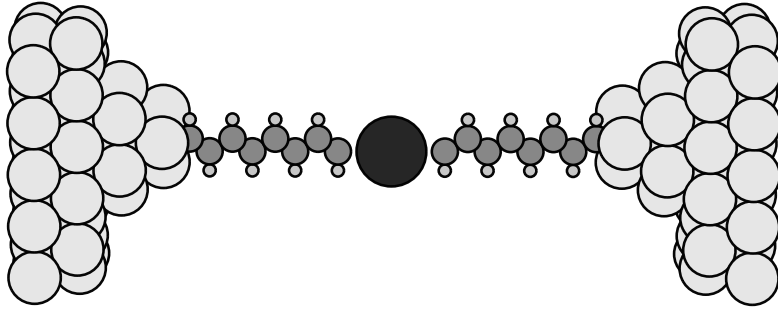
FIG. 2. Band structure for conjugated polyacetylene calculated using extended Hückel. The  $\pi$  band extends from -14.5 eV to -5 eV and has a band gap starting at -11.2 eV.



Emberly & Kirczenow Fig. 3

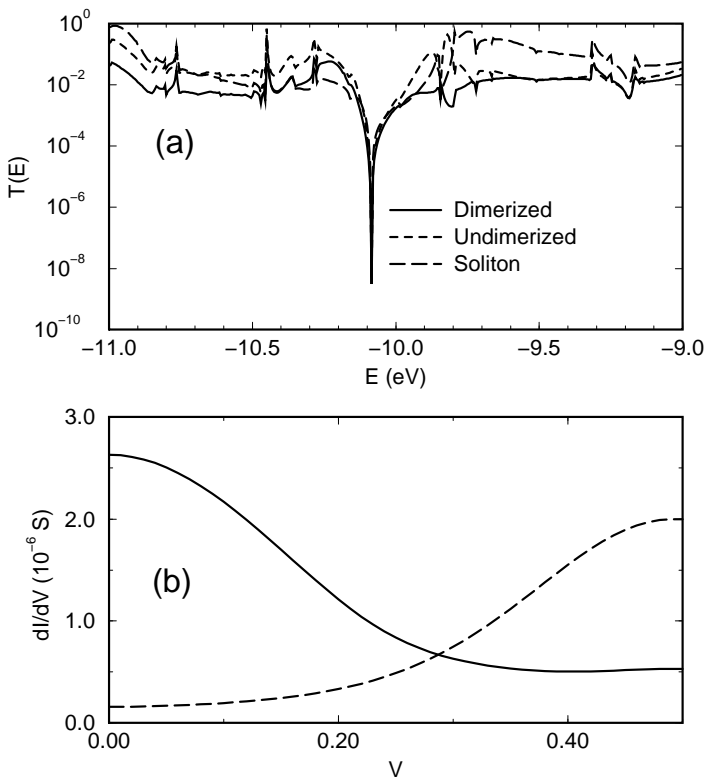
ht]

FIG. 3. (Solid line) transmission plot for a molecule with a single  $\pi$  state connected to polyacetylene leads. (Dashed line) transmission plot calculated using analytic theory for similar system.



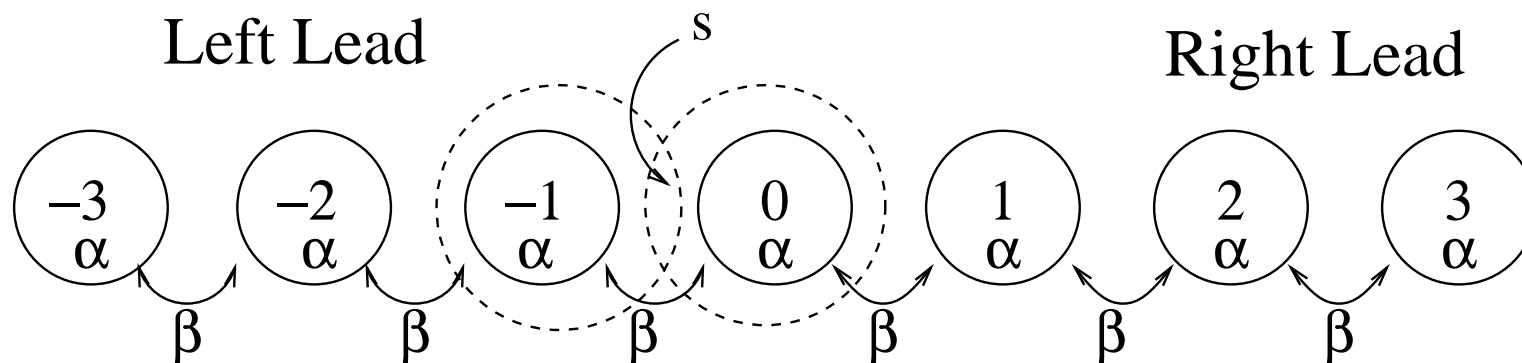
Emberly & Kirczenow Fig. 4

FIG. 4. Atomistic diagram for the MCBJ and molecular wire system. The first unit cells of the left and right (111) leads are shown as the last two layers of gold atoms on either side. Also shown are the  $(\text{CH})_8$  chain molecules and “active” molecule. These are attached to two clusters of 10 gold atoms that form the tip. The perpendicular distance between the the last C atoms on the chains and the triangle of gold atoms is 1.6 Angstroms.



Emberly and Kirczenow Fig. 5

FIG. 5. (a) The calculated transmission for a two state active molecule attached to CH chains and gold (111) contacts. (b) The calculated differential conductance assuming a Fermi energy of (solid line) -10.2 eV and (dashed line) -10.0 eV and a temperature of  $T = 293$  K.



Emberly & Kirczenow Fig. 6